

# Spectral Absorption from Two-view Hyperspectral Images

Kenta Kageyama, Ryo Kawahara<sup>a</sup> and Takahiro Okabe<sup>b</sup>

Department of Artificial Intelligence, Kyushu Institute of Technology,  
680-4 Kawazu, Iizuka, Fukuoka 820-8502, Japan

**Keywords:** Spectral Imaging, Passive Measurement, Spectral Absorption Coefficient, Matrix Factorization.

**Abstract:** When light passes through a liquid, its energy is attenuated due to absorption. The attenuation depends both on the spectral absorption coefficient of a liquid and on the optical path length of light, and is described by the Lambert-Beer law. The spectral absorption coefficients of liquids are often unknown in real-world applications and to be measured/estimated in advance, because they depend not only on liquid media themselves but also on dissolved materials. In this paper, we propose a method for estimating the spectral absorption coefficient of a liquid only from two-view hyperspectral images of an under-liquid scene taken from the outside of the liquid in a passive and non-contact manner. Specifically, we show that the estimation results in Non-negative Matrix Factorization (NMF) because both the objective variables and the explanatory variables are all non-negative, and then study the ambiguity in matrix factorization. We conducted a number of experiments using real hyperspectral images, and confirmed that our method works well and is useful for reconstructing shape of an under-liquid scene.

## 1 INTRODUCTION


When light passes through a liquid, a part of the light is often absorbed and scattered by the liquid, and then its energy is attenuated in general. For transparent liquids with negligible scattering, it is known that the attenuation of light energy due to absorption depends both on the *spectral absorption coefficient* of a liquid and on the optical path length of light in the liquid, and is described by the Lambert-Beer law (Reinhard et al., 2008).


The absorption due to liquid is an important clue to solving computer vision problems; shape recovery of underwater objects (Asano et al., 2016; Murai et al., 2019; Takatani et al., 2021; Kuo et al., 2021) and liquid detection on unknown surfaces (Wang et al., 2021; Wang and Okabe, 2021) are achieved under the assumption that the spectral absorption coefficients of liquids are known. Unfortunately, however, the spectral absorption coefficients of liquids are often unknown in real-world applications and to be measured/estimated in advance, because they depend not only on liquid media themselves but also on dissolved materials.

Conventionally, the spectral absorption coeffi-

icients of liquids are measured via absorption spectroscopy (Jones and Kao, 1969; Kao and Davies, 1968) in an *active and contact* manner. Specifically, when the Spectral Power Distributions (SPDs) of the light both before and after transmitting a liquid of interest are known, its spectral absorption coefficient is derived from the logarithm of the ratio of those SPDs on the basis of the Lambert-Beer law. In the above computer vision problems with hyperspectral images of a scene, however, the SPD of the light before transmitting a liquid, *i.e.* the spectral radiance on an object surface under the liquid is unknown.

Accordingly, we propose a method for estimating the spectral absorption coefficients of liquids in a *passive and non-contact* manner. Our proposed method estimates the spectral absorption coefficient of a liquid only from two-view hyperspectral images of an under-liquid scene taken from the outside of the liquid. We make use of the fact that the absorption coefficient depends on the wavelengths but the optical path length depends on the scene points. Specifically, our method estimates the spectral absorption coefficient on the basis of Non-negative Matrix Factorization (NMF) (Berry et al., 2007), because both the objective variables described by the observed spectral radiance values and the explanatory variables described by the spectral absorption coefficients, optical path lengths, and Fresnel terms are all non-negative.

<sup>a</sup>  <https://orcid.org/0000-0002-9819-3634>

<sup>b</sup>  <https://orcid.org/0000-0002-2183-7112>

Moreover, we study the ambiguity of our proposed method based on matrix factorization. We show that our method using only two-view hyperspectral images can estimate the spectral absorption coefficient up to a scale and an offset. We also show that the estimated spectral absorption coefficient is useful for shape recovery even though it has the ambiguity; we show that the shape of an object surface under liquid is recovered up to a scale.

The main contributions of this paper are threefold. First, we propose a novel method for estimating the spectral absorption coefficient of a liquid in a passive and non-contact manner. The proposed method achieves the estimation of a spectral absorption coefficient only from two-view hyperspectral images without requiring the SPD of the light before transmitting a liquid. Second, we show that our method can estimate the spectral absorption coefficient up to a scale and an offset. In addition, we show that the spectral absorption coefficient with the ambiguity is useful for under-liquid shape recovery. Third, we conducted a number of experiments using real hyperspectral images, and confirmed that our method works well and is useful for reconstructing shape of an under-liquid scene.

## 2 RELATED WORK

### 2.1 Absorption Measurement

Absorption spectroscopy (Jones and Kao, 1969; Kao and Davies, 1968) is a classical method for measuring the spectral absorption coefficient of a liquid of interest in an active and contact manner. When the SPDs of the light both before and after transmitting the liquid are known, its spectral absorption coefficient is derived from the logarithm of the ratio of those SPDs on the basis of the Lambert-Beer law (Reinhard et al., 2008). In the computer vision problems with hyperspectral images of a scene such as shape recovery (Asano et al., 2016; Murai et al., 2019; Takatani et al., 2021; Kuo et al., 2021) and liquid detection (Wang et al., 2021; Wang and Okabe, 2021), however, the SPD of the light before transmitting a liquid, *i.e.* the spectral radiance on an object surface under the liquid is unknown. Therefore, we achieve the estimation of the spectral absorption coefficient of a liquid only from two-view hyperspectral images without requiring the SPD of the light before transmitting the liquid.

In the community of computer vision, the three-band (RGB) attenuation coefficient, *i.e.* the summation of the absorption and scattering coefficients

of a liquid is often measured or estimated. It is known that the attenuation coefficient can be estimated from an image of a known calibration target at known distances (Tsiotsios et al., 2014; Murez et al., 2015; Akkaynak and Treibitz, 2019), but such estimation requires external hardware and distance measurement. The attenuation/absorption coefficient can be estimated from multiple images of the same object located at different distances; the distances are assumed to be known (Yamashita et al., 2007), or measured by a sonar (Kaeli et al., 2011), or recovered via structure from motion (Jordt-Sedlazeck and Koch, 2013; Bryson et al., 2016). In contrast, our proposed method estimates the spectral absorption coefficient only from two-view hyperspectral images with neither a known calibration target nor know distances nor geometric calibration.

### 2.2 Computer Vision Applications

The absorption due to liquid is an important clue to shape recovery. Asano *et al.* (Asano et al., 2016) make use of the fact that water absorbs Near InfraRed (NIR) light (Curcio and Petty, 1951), and show that the shape (depth) of an under-water scene can be recovered from two single-view images at different wavelengths in NIR range. Takatani *et al.* (Takatani et al., 2021) extends the above method by using an event-based camera with temporally modulated illumination, and then achieve robust shape reconstruction in water. Murai *et al.* (Murai et al., 2019) reconstruct both the surface normals and depth of a dynamic object in water by using multi-directional NIR lighting. Furthermore, Kuo *et al.* (Kuo et al., 2021) achieve shape reconstruction of a dynamic and non-rigid object in water.

The absorption due to liquid is useful also for liquid detection. Wang *et al.* (Wang et al., 2021) make use of the fact that the absorption due to water decreases the apparent spectral reflectance on an object surface. They achieve per-pixel water detection on surfaces with unknown reflectance by using the low-dimensional linear model of spectral reflectance from visible to NIR wavelengths. Further, Wang and Okabe (Wang and Okabe, 2021) extends their method to water and oil detection on unknown surfaces by simultaneously estimating the types of liquids and optical path lengths.

The above applications assume that the spectral absorption coefficients of liquids of interest (water and oils) are known. Unfortunately, however, the spectral absorption coefficients of liquids are often unknown in real-world applications and to be measured/estimated in advance. The spectral absorption

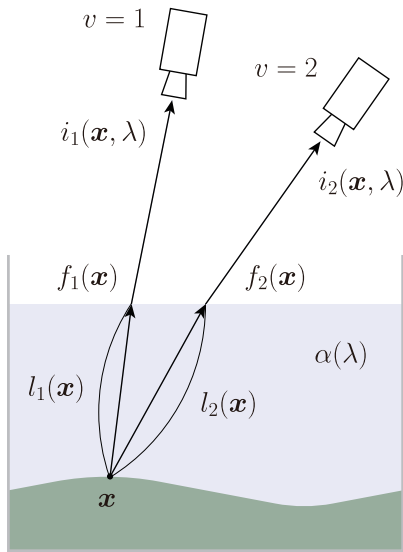


Figure 1: The illustration of our setup for spectral absorption recovery; our proposed method uses two-view hyperspectral images of an under-liquid scene taken from the outside of the liquid.

coefficients estimated by using our proposed method in a passive and non-contact manner are effective for those computer vision applications.

### 3 PROPOSED METHOD

We propose a method for estimating the spectral absorption coefficient of a liquid of interest in a passive and non-contact manner. As shown in Figure 1, our proposed method uses two-view hyperspectral images of an under-liquid scene taken from the outside of the liquid. We assume that the liquid is spatially uniform and transparent with negligible scattering and that the attenuation of light energy due to absorption obeys the Lambert-Beer law.

When we observe a point  $\mathbf{x}$  on an under-liquid object surface from the  $v$ -th ( $v = 1, 2$ ) viewpoint, the spectral radiance  $i_v(\mathbf{x}, \lambda)$  of the point  $\mathbf{x}$  at the wavelength  $\lambda$  seen through the liquid is given by

$$i_v(\mathbf{x}, \lambda) = f_v(\mathbf{x})r_v(\mathbf{x}, \lambda)e^{-\alpha(\lambda)l_v(\mathbf{x})} \quad (1)$$

according to the Lambert-Beer law (Reinhard et al., 2008). Here,  $f_v(\mathbf{x})$ ,  $r_v(\mathbf{x}, \lambda)$ ,  $\alpha(\lambda)$ , and  $l_v(\mathbf{x})$  are the Fresnel term<sup>1</sup>, the spectral radiance of the point before transmitting the liquid, the spectral absorption

<sup>1</sup>We assume that the Fresnel term is independent of the wavelength of light. Actually, the Fresnel term depends on the wavelength via the refractive index, but the refractive indexes of liquids such as water are almost constant for visible wavelengths.

coefficient of the liquid, and the optical path length in the liquid.

Taking the logarithm of the ratio between  $i_1(\mathbf{x}, \lambda)$  and  $i_2(\mathbf{x}, \lambda)$ , we obtain

$$\begin{aligned} \ln \frac{i_1(\mathbf{x}, \lambda)}{i_2(\mathbf{x}, \lambda)} &= \ln \frac{f_1(\mathbf{x})r_1(\mathbf{x}, \lambda)e^{-\alpha(\lambda)l_1(\mathbf{x})}}{f_2(\mathbf{x})r_2(\mathbf{x}, \lambda)e^{-\alpha(\lambda)l_2(\mathbf{x})}} \\ &= \alpha(\lambda)\{l_2(\mathbf{x}) - l_1(\mathbf{x})\} + \ln \frac{f_1(\mathbf{x})}{f_2(\mathbf{x})}. \end{aligned} \quad (2)$$

Here, we assume that the under-liquid object surface obeys the Lambert model, and therefore the spectral radiance is independent of viewpoints:  $r_1(\mathbf{x}, \lambda) = r_2(\mathbf{x}, \lambda)$ .

The above equation holds for the corresponding point  $\mathbf{x}_p$  ( $p = 1, 2, 3, \dots, P$ ) between the two-view hyperspectral images with the wavelength  $\lambda_w$  ( $w = 1, 2, 3, \dots, W$ ). Then, we can rewrite eq.(2) by using matrices as

$$\mathbf{S} = \mathbf{A}\mathbf{B}. \quad (3)$$

Here, the  $W \times P$  observation matrix  $\mathbf{S}$ , the  $W \times 2$  matrix  $\mathbf{A}$  depending on the wavelengths, and the  $2 \times P$  matrix  $\mathbf{B}$  depending on the scene points are given by

$$\mathbf{S} = \begin{pmatrix} s_{11} & s_{12} & \cdots & s_{1P} \\ s_{21} & s_{22} & \cdots & s_{2P} \\ \vdots & \vdots & \ddots & \vdots \\ s_{W1} & s_{W2} & \cdots & s_{WP} \end{pmatrix}, \quad (4)$$

$$\mathbf{A} = \begin{pmatrix} \alpha_1 & 1 \\ \alpha_2 & 1 \\ \vdots & \vdots \\ \alpha_W & 1 \end{pmatrix}, \quad (5)$$

$$\mathbf{B} = \begin{pmatrix} l'_1 & l'_2 & \cdots & l'_P \\ f'_1 & f'_2 & \cdots & f'_P \end{pmatrix}, \quad (6)$$

where  $s_{wp} = \ln\{i_1(\mathbf{x}_p, \lambda_w)/i_2(\mathbf{x}_p, \lambda_w)\}$ ,  $\alpha_w = \alpha(\lambda_w)$ ,  $l'_p = l_2(\mathbf{x}_p) - l_1(\mathbf{x}_p)$ , and  $f'_p = \ln\{f_1(\mathbf{x}_p)/f_2(\mathbf{x}_p)\}$ .

When we take the first/second images from deep/shallow angles as shown in Figure 1, we can assume that  $i_1(\mathbf{x}_p, \lambda_w) \geq i_2(\mathbf{x}_p, \lambda_w)$ ,  $l_2(\mathbf{x}_p) \geq l_1(\mathbf{x}_p)$ , and  $f_1(\mathbf{x}_p) \geq f_2(\mathbf{x}_p)$ . Then, all the elements in the matrices  $\mathbf{S}$ ,  $\mathbf{A}$ , and  $\mathbf{B}$  in eq.(3) are non-negative. Therefore, the estimation of the spectral absorption coefficient results in NMF: factorizing the non-negative observation matrix  $\mathbf{S}$  into the product of the non-negative matrices  $\mathbf{A}$  and  $\mathbf{B}$ . Hence, our method can estimate not only the spectral absorption coefficient  $\alpha(\lambda_w)$  but also the difference of the optical path lengths  $l_2(\mathbf{x}_p) - l_1(\mathbf{x}_p)$  and the ratio of the Fresnel term  $f_1(\mathbf{x}_p)/f_2(\mathbf{x}_p)$  as byproducts.

In our current implementation, we factorize the observation matrix via alternative least squares (Berry

et al., 2007). Specifically, we minimize the sum of squares

$$\sum_{w,p} (s_{wp} - \alpha_w l'_p - f'_p)^2 \quad (7)$$

with respect to the non-negative unknown variable  $\alpha_w$ ,  $l'_p$ , and  $f'_p$ . We give random initial values for  $\{l'_p, f'_p\}$ , and then iteratively fix one set of variables ( $\{l'_p, f'_p\}$  or  $\alpha_w$ ) and update the other set of variables via least squares and vice versa.

## 4 AMBIGUITY ANALYSIS

### 4.1 Ambiguity in Matrix Factorization

In general, matrix factorization has ambiguity. Since our proposed method results in the factorization of the  $W \times P$  observation matrix  $\mathbf{S}$  into the  $W \times 2$  matrix  $\mathbf{A}$  and the  $2 \times P$  matrix  $\mathbf{B}$ , the ambiguity is represented by using a  $2 \times 2$  arbitrary invertible matrix  $\mathbf{C}$  as

$$\mathbf{S} = \mathbf{A}\mathbf{B} = \mathbf{A}\mathbf{C}\mathbf{C}^{-1}\mathbf{B} = (\mathbf{A}\mathbf{C})(\mathbf{C}^{-1}\mathbf{B}). \quad (8)$$

In other words, the matrices  $\{\mathbf{A}, \mathbf{B}\}$  and the matrices  $\{\mathbf{A}\mathbf{C}, \mathbf{C}^{-1}\mathbf{B}\}$  yield the same matrix  $\mathbf{S}$ .

Then, from eq.(5), the relationship between the spectral absorption coefficient estimated by our proposed method  $\hat{\alpha}_w = \hat{\alpha}(\lambda_w)$  and its ground truth  $\alpha_w = \alpha(\lambda_w)$  is given by

$$\begin{aligned} \begin{pmatrix} \hat{\alpha}_1 & 1 \\ \hat{\alpha}_2 & 1 \\ \vdots & \vdots \\ \hat{\alpha}_W & 1 \end{pmatrix} &= \begin{pmatrix} \alpha_1 & 1 \\ \alpha_2 & 1 \\ \vdots & \vdots \\ \alpha_W & 1 \end{pmatrix} \begin{pmatrix} c_{11} & c_{12} \\ c_{21} & c_{22} \end{pmatrix} \\ &= \begin{pmatrix} c_{11}\alpha_1 + c_{21} & c_{12}\alpha_1 + c_{22} \\ c_{11}\alpha_2 + c_{21} & c_{12}\alpha_2 + c_{22} \\ \vdots & \vdots \\ c_{11}\alpha_W + c_{21} & c_{12}\alpha_W + c_{22} \end{pmatrix}. \end{aligned} \quad (9)$$

Here,  $c_{ij}$  is the element of the matrix  $\mathbf{C}$  at the  $i$ -th row and  $j$ -th column.

We can derive that  $c_{12} = 0$  and  $c_{22} = 1$  from the above equation, because the spectral absorption coefficients are not constant with respect to wavelengths in general. Therefore, the ambiguity of our proposed method is represented by the  $2 \times 2$  invertible matrix  $\mathbf{C}$  defined by

$$\mathbf{C} = \begin{pmatrix} c_{11} & 0 \\ c_{21} & 1 \end{pmatrix}. \quad (10)$$

Thus, our method can estimate the spectral absorption coefficient up to an unknown scale  $c_{11}$  and an unknown offset  $c_{21}$ :

$$\hat{\alpha}(\lambda) = c_{11}\alpha(\lambda) + c_{21}. \quad (11)$$

### 4.2 Ambiguity in Shape Recovery

Asano *et al.* (Asano et al., 2016) show that the shape (depth) of an under-water scene can be recovered from two single-view images at different wavelengths  $\lambda_1$  and  $\lambda_2$ . Specifically, the depth  $l(\mathbf{x})$  of a surface point  $\mathbf{x}$  is described as

$$l(\mathbf{x}) = \frac{1}{2\{\alpha(\lambda_2) - \alpha(\lambda_1)\}} \ln \frac{i(\mathbf{x}, \lambda_1)}{i(\mathbf{x}, \lambda_2)}, \quad (12)$$

where  $i(\mathbf{x}, \lambda_1)$  and  $i(\mathbf{x}, \lambda_2)$  are the spectral radiance values seen through water with the two wavelengths. Therefore, the depth of an under-liquid (under-water in this case) scene can be recovered if the spectral absorption coefficient of the liquid is known.

We show that the spectral absorption coefficient estimated by our proposed method can be used for reconstructing the shape of an under-liquid scene. Replacing the ground truth spectral absorption coefficient in eq.(12) with the estimated one in eq.(11), the estimated depth  $\hat{l}(\mathbf{x})$  is given by

$$\begin{aligned} \hat{l}(\mathbf{x}) &= \frac{1}{2\{\hat{\alpha}(\lambda_2) - \hat{\alpha}(\lambda_1)\}} \ln \frac{i(\mathbf{x}, \lambda_1)}{i(\mathbf{x}, \lambda_2)} \\ &= \frac{1}{c_{11}} l(\mathbf{x}). \end{aligned} \quad (13)$$

This is because the offset  $c_{21}$  in the denominator is canceled out due to subtraction. Hence, the shape of an under-liquid scene can be recovered up to an unknown scale.

## 5 EXPERIMENTS

### 5.1 Setup

To confirm the effectiveness of our proposed method, we conducted a number of experiments using real hyperspectral images. We tested three scenes in an acrylic tank: (A) a textured board in dilute methylene blue, (B) gravel in dilute methylene blue, and (C) gravel in dilute soy sauce. We captured those scenes from the outside of the tank as shown in Figure 2. We used a halogen lamp and a hyperspectral camera from EBA Japan that can capture the range of near UV (380 nm) to near IR (1,000 nm) with the interval of 5 nm, *i.e.* 125 spectral channels in total.

### 5.2 Spectral Absorption Coefficient

First, we studied the performance of our proposed method by comparing the estimated spectral absorption coefficients with their ground truths. We measured the ground truth of the spectral absorption coefficient of a liquid from the hyperspectral images of a



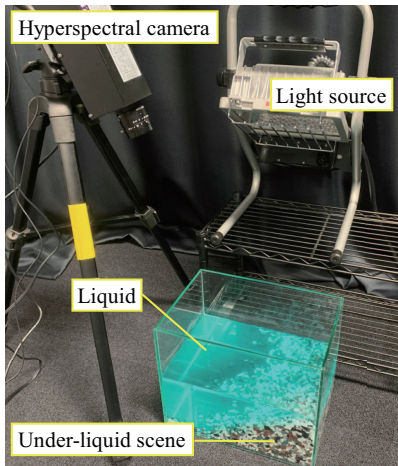


Figure 2: Our setup for spectral absorption recovery; we captured an under-liquid scene in an acrylic tank from the outside by using a hyperspectral camera.

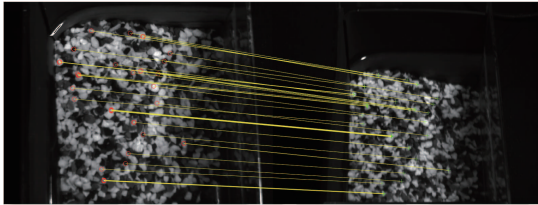


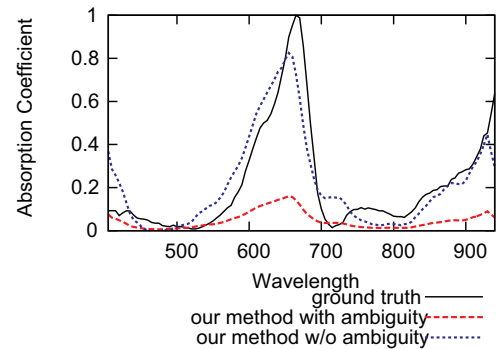
Figure 3: The two-view images of (B) the gravel in dilute methylene blue at 530 nm and the corresponding points between them.

target object seen through the liquid with known and variable depths.

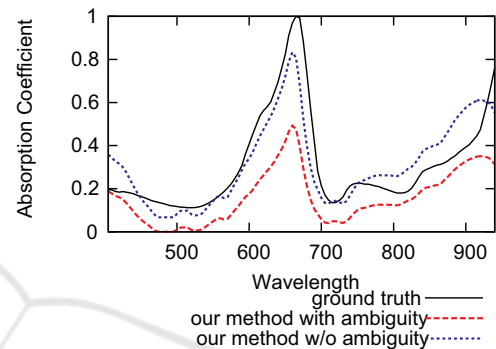
As described in Section 3, our proposed method requires the correspondence between two hyperspectral images taken from different viewpoints. In our current implementation, we used MSER (Maximally Stable Extremal Regions) features (Matas et al., 2004) in MATLAB in order to achieve the correspondence between those images. Figure 3 shows the two-view images of (B) the gravel in dilute methylene blue at 530 nm and the corresponding points between them. In general, the minimization of the sum of squares in eq.(7) depends on the random initial values. In our current implementation, we tested 100 sets of random initial values, and found out the best solution with the minimum sum of squares.

Figure 4 shows the spectral absorption coefficients; (a), (b), and (c) show the results of the three scenes (A), (B), and (C). The black solid line, the red dashed line, and the blue dotted line stand for the ground truth<sup>2</sup>, the estimated one with the ambiguity,

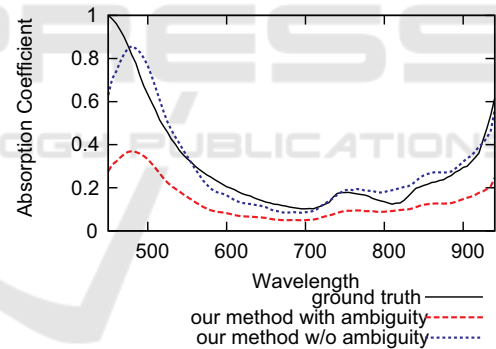
<sup>2</sup>We normalize the ground truth of a spectral absorption coefficient so that its maximum value with respect to wavelength is equal to 1.



(a)



(b)



(c)

Figure 4: The spectral absorption coefficients; (a), (b), and (c) show the results of the three scenes (A), (B), and (C). The black solid line, the red dashed line, and the blue dotted line stand for the ground truth, the estimated one with and without the ambiguity.

and the estimated one without the ambiguity, *i.e.* with the optimal scale and offset respectively. Since our proposed method can estimate the spectral absorption coefficient up to a scale and an offset, we supposed that the ground truth is known and computed the optimal ones via least squares for comparison. The range of the wavelength within which the spectral absorption coefficient is estimated is different; from 405 nm to 940 nm for the dilute methylene blue and from 450 nm to 940 nm for the dilute soy sauce. This is because

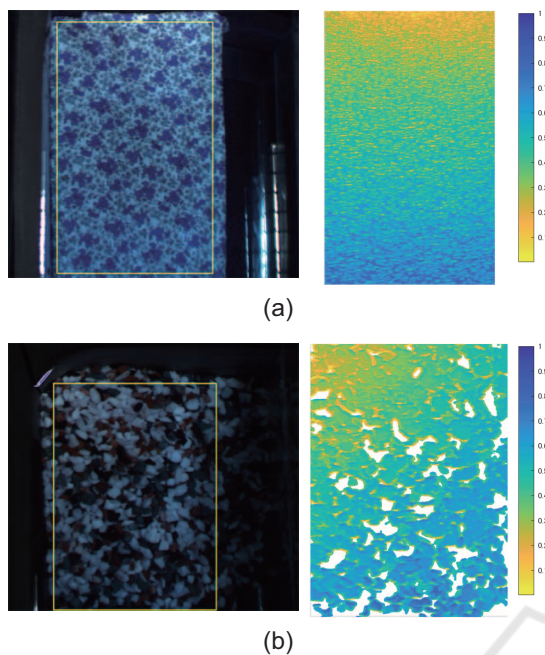


Figure 5: The pseudo color images (left) and the reconstructed depth maps (right) within the yellow boxes; (a) and (b) show the results of the two scenes (A) and (B).

we could not estimate the spectral absorption coefficient at some wavelengths where the observed spectral radiance values are too small due to weak light source and/or strong absorption.

Comparing the ground truths and the estimated absorption coefficients with the ambiguity in Figure 4, we can see that the estimated ones capture the properties of the liquids; the dilute methylene blue absorbs red and green wavelengths and looks bluish<sup>3</sup>, and the dilute soy sauce absorbs blue and green wavelengths and looks reddish. Since both the liquids are diluted by water, we can see the absorption due to water in NIR wavelengths. Then, we can see that the estimated absorption coefficients with the optimal scale and offset are almost the same as the ground truths. The RMS (Root-Mean-Square) errors of the spectral absorption coefficients are 0.108, 0.108, and 0.070 for (a) the first dilute methylene blue, (b) the second dilute methylene blue, and (c) the dilute soy sauce respectively. Those results show that our method can accurately estimate the spectral absorption coefficients up to a scale and an offset.

<sup>3</sup>The spectral absorption coefficients of the methylene blue in (a) and (b) are different because their concentrations are different.

### 5.3 Application to Shape Recovery

Second, we studied the effectiveness of the estimated spectral absorption coefficient with the ambiguity for under-liquid shape recovery. According to Asano *et al.* (Asano *et al.*, 2016), we placed the hyperspectral camera and the light source at almost the same location. In addition, their method assumes that, at two wavelengths  $\lambda_1$  and  $\lambda_2$  in eq.(13), the spectral reflectances are almost the same, but the spectral absorption coefficients are significantly different. It is known that the spectral reflectances of most materials are almost constant for NIR wavelengths (Choe *et al.*, 2016). Therefore, we chose the two wavelengths  $\lambda_1 = 825$  nm and  $\lambda_2 = 900$  nm where the spectral absorption coefficients are significantly different as shown in Figure 4.

Figure 5 shows the pseudo color images (left) and the reconstructed depth maps (right) within the yellow boxes; (a) and (b) show the results of the two scenes (A) and (B). Here, the color bar shows the relationship between the relative depth and the color from shallow (yellow) to deep (blue). The white pixels in those depth maps stand for the pixels where the reflectance is low and then the radiance values are too small to estimate the depth. We can see that the reconstructed depth maps qualitatively show the effectiveness of the estimated spectral absorption coefficient with the ambiguity; the depth of the textured board increases linearly from the top to the bottom, and the depth of gravel gradually increases from the top left to the bottom right in the images.

## 6 CONCLUSION AND FUTURE WORK

In this paper, we proposed a novel method for estimating the spectral absorption coefficient of a liquid only from two-view hyperspectral images of an under-liquid scene taken from the outside of the liquid in a passive and non-contact manner. Specifically, we showed that the estimation results in NMF, and then studied the ambiguity in matrix factorization. We conducted a number of experiments using real hyperspectral images, and confirmed that our method works well and is useful for reconstructing shape of an under-liquid scene.

Our future work includes the extension to scattering medium: the estimation of absorption and scattering coefficients. The integration of spectral imaging with polarimetric imaging (Schechner and Karpel, 2004) and the use of the prior knowledge with respect to attenuation/absorption coefficients (Akkay-

nak et al., 2017) are other directions of our future study. In addition, the integration of camera-based spectral imaging with illumination-based spectral imaging (Kitahara et al., 2015; Kobayashi and Okabe, 2016; Wang and Okabe, 2017; Torii et al., 2019; Koyamatsu et al., 2019) is an interesting direction to be addressed.

## ACKNOWLEDGEMENTS

This work was supported by JSPS KAKENHI Grant Number JP20H00612.

## REFERENCES

- Akkaynak, D. and Treibitz, T. (2019). Sea-thru: A method for removing water from underwater images. In *Proc. IEEE/CVF CVPR2019*, pages 1682–1691.
- Akkaynak, D., Treibitz, T., Shlesinger, T., Loya, Y., Tamir, R., and Iluz, D. (2017). What is the space of attenuation coefficients in underwater computer vision? In *Proc. IEEE CVPR2017*, pages 568–577.
- Asano, Y., Zheng, Y., Nishino, K., and Sato, I. (2016). Shape from water: Bispectral light absorption for depth recovery. In *Proc. ECCV2016*, pages 635–649.
- Berry, M., Browne, M., Langville, A., Pauca, V., and Plemmons, R. (2007). Algorithms and applications for approximate nonnegative matrix factorization. *Computational Statistics & Data Analysis*, 52(1):155–173.
- Bryson, M., Johnson-Roberson, M., Pizarro, O., and Williams, S. B. (2016). True color correction of autonomous underwater vehicle imagery. *Journal of Field Robotics*, 33(6):853–874.
- Choe, G., Narasimhan, S. G., and Kweon, I. S. (2016). Simultaneous estimation of near IR BRDF and fine-scale surface geometry. In *Proc. IEEE CVPR2016*, pages 2452–2460.
- Curcio, J. A. and Petty, C. C. (1951). The near infrared absorption spectrum of liquid water. *JOSA A*, 41(5):302–304.
- Jones, M. W. and Kao, K. C. (1969). Spectrophotometric studies of ultra low loss optical glasses II: double beam method. *Journal of Physics E: Scientific Instruments*, 2(4):331–335.
- Jordt-Sedlazeck, A. and Koch, R. (2013). Refractive structure-from-motion on underwater images. In *Proc. IEEE ICCV2013*, pages 57–64.
- Kaeli, J. W., Singh, H., Murphy, C., and Kunz, C. (2011). Improving color correction for underwater image surveys. In *Proc. MTS/IEEE OCEANS2011*, pages 1–6.
- Kao, K. C. and Davies, T. W. (1968). Spectrophotometric studies of ultra low loss optical glasses I: single beam method. *Journal of Physics E: Scientific Instruments*, 1(11):1063–1068.
- Kitahara, M., Okabe, T., Fuchs, C., and Lensch, H. P. A. (2015). Simultaneous estimation of spectral reflectance and normal from a small number of images. In *Proc. VISAPP2015*, pages 303–313.
- Kobayashi, N. and Okabe, T. (2016). Separating reflection components in images under multispectral and multi-directional light sources. In *Proc. IAPR ICPR2016*, pages 3199–3204.
- Koyamatsu, K., Hidaka, D., Okabe, T., and Lensch, H. P. A. (2019). Reflective and fluorescent separation under narrow-band illumination. In *Proc. IEEE/CVF CVPR2019*, pages 7577–7585.
- Kuo, M.-Y. J., Kawahara, R., Nobuhara, S., and Nishino, K. (2021). Non-rigid shape from water. *IEEE TPAMI*, 43(7):2220 – 2232.
- Matas, J., Chum, O., Urban, M., and Pajdla, T. (2004). Robust wide-baseline stereo from maximally stable extremal regions. *Image and Vision Computing*, 22(10):761–767.
- Murai, S., Kuo, M., Kawahara, R., Nobuhara, S., and Nishino, K. (2019). Surface normals and shape from water. In *Proc. IEEE/CVF ICCV2019*, pages 7829–7837.
- Murez, Z., Treibitz, T., Ramamoorthi, R., and Kriegman, D. (2015). Photometric stereo in a scattering medium. In *Proc. IEEE ICCV2015*, pages 3415–3423.
- Reinhard, E., Khan, E. A., Akyuz, A. O., and Johnson, G. (2008). *Color Imaging: Fundamentals and Applications*. A K Peters/CRC Press.
- Schechner, Y. Y. and Karpel, N. (2004). Clear underwater vision. In *Proc. IEEE CVPR2004*, pages 536–543.
- Takatani, T., Ito, Y., Ebisu, A., Zheng, Y., and Aoto, T. (2021). Event-based bispectral photometry using temporally modulated illumination. In *Proc. IEEE/CVF CVPR2021*, pages 15638–15647.
- Torii, M., Okabe, T., and Amano, T. (2019). Multispectral direct-global separation of dynamic scenes. In *Proc. IEEE WACV2019*, pages 1923–1931.
- Tsiotsios, C., Angelopoulou, M. E., Kim, T.-K., and Davison, A. J. (2014). Backscatter compensated photometric stereo with 3 sources. In *Proc. IEEE ICCV2014*, pages 2259–2266.
- Wang, C. and Okabe, T. (2017). Joint optimization of coded illumination and grayscale conversion for one-shot raw material classification. In *Proc. BMVC2017*.
- Wang, C. and Okabe, T. (2021). Per-pixel water and oil detection on surfaces with unknown reflectance. In *Proc. EUSIPCO2021*, pages 601–605.
- Wang, C., Okuyama, M., Matsuoka, R., and Okabe, T. (2021). Per-pixel water detection on surfaces with unknown reflectance. *IEICE Trans. Information and Systems*, E104-D(10):1555–1562.
- Yamashita, A., Fujii, M., and Kaneko, T. (2007). Color registration of underwater images for underwater sensing with consideration of light attenuation. In *Proc. IEEE ICRA2007*, pages 4570–4575.